Conformation, Molecular Packing, and Field Effect Mobility of Regioregular *β,β′*-Dihexylsexithiophene

Nataliya Kiriy,[†] Anton Kiriy,*[,‡] Vera Bocharova,[‡] Manfred Stamm,[‡] Stephan Richter,[§] Matthias Plötner,[§] Wolf-Joachim Fischer,[§] Frederik C. Krebs,[∥] Irena Senkovska,[⊥] and Hans-Juergen Adler[†]

Institute of Macromolecule Chemistry and Textile Chemistry, Mommsenstrasse 13, 01062 Dresden, Germany, Institute of Polymer Research, Hohe Strasse 6, 01069 Dresden, Germany, Institute of Semiconductor and Microsystems Technology, Nothnitzer Strasse 64, 01062 Dresden, Germany, The Danish Polymer Centre, RISØ National Laboratory, P.O. Box 49, DK-4000 Roskilde, Denmark, and Sector for X-ray and Electron Diffraction, University of Ulm, D-89081 Ulm, Germany

Received February 27, 2004. Revised Manuscript Received April 28, 2004

Improved synthesis, charge carrier mobility, conformation, crystalline structure, and molecular packing of the regiochemically pure 4′,3‴″-dihexyl-2,2′;5′,2″;5″,2‴;5‴,2⁗;5⁗,2⁗′-sexithiophene (*β,β′*-DH6T) are reported. The sum of charge carrier mobilities of *β,β′*-DH6T measured by the pulse-radiolysis time-resolved microwave conductivity (PR-TRMC) technique was found to be $\sum\mu_{min} = 3.9 \times 10^{-3}$ cm^2 V^{-1} s^{-1}, which is comparable with the PR-TRMC mobility found for α,*ω*-DH6T. The field-effect mobility (FEM) of *β,β′*-DH6T was found to be on the order of 10^{-5} cm^2 V^{-1} s^{-1}, which is considerably less than the FEM of α,*ω*-DH6T. To understand the reason for such poor macroscopic electrical properties, the conformation and the molecular packing of *β,β′*-DH6T were systematically studied by means of UV−vis spectroscopy, scanning electron microscopy (SEM), atomic force microscopy (AFM), and X-ray techniques. Absorption spectra of a *β,β′*-DH6T spin-cast film indicate the planar conformation of the aromatic backbone. SEM and AFM reveal the formation of an ordered lamellar phase. As a single-crystal X-ray study shows, *β,β′*-DH6T exhibits less dense crystalline packing than α,*ω*-DH6T. In contrast to the almost upright orientation of α,*ω*-DH6T molecules against the substrate (tilt angle about 68°), the long axis of *β,β′*-DH6T molecules and the surface plane form an angle of ∼20°. Thus, the crystalline structure of α,*ω*-DH6T "allows" the current to flow along the molecular stacks; the crystalline structure of *β,β′*-DH6T suppresses the charge transport.

Introduction

π-Conjugated polymers and oligomers are well-known for their interesting electronic and photonic properties.[1] Although the performance of organic thin-film field-effect transistors (FETs) made from such materials has been significantly improved during the past few years, some important problems still exist that hinder their industrial application.[1,2] Therefore, a design of novel organic semiconductors which combine high environmental stability, good solubility, and appropriate charge transport properties is highly desirable.

Oligothiophenes (OTs) represent one of the most promising classes of semiconductive materials for FET fabrication because of their good mobility and environmental stability.[2−4] However, unsubstituted OTs are insoluble in the usual solvents and can be deposited only by vacuum evaporation, which is expensive and problematic from an industrial point of view. The high charge mobility and poor solubility of sexithiophene (6T) are linked through the great molecular ordering and side-by-side stacking of aromatic molecules. It has been shown that the introduction of alkyl groups in the α- and *ω*-positions[5] or short substituents (methyl groups)

* To whom correspondence should be addressed. E-mail: kiriy@ipfdd.de. Phone: +49-351-4658-294. Fax: +49-351-4658-284.
[†] Institute of Macromolecule Chemistry and Textile Chemistry.
[‡] Institute of Polymer Research.
[§] Institute of Semiconductor and Microsystems Technology.
[∥] RISØ National Laboratory.
[⊥] University of Ulm.

(1) Skotheim, T. A.; Elsenbaumer, R. L.; Reynolds, J. R. *Handbook of Conducting Polymers*; Marcel Dekker: New York, 1998.
(2) Dimitropoulos, C. D.; Malenfant, P. R. L. *Adv. Mater.* **2002**, *14*, 99. Sirringhaus, H.; Kawase, T.; Friend, R. H.; Shimoda, T.; Inbasekaran, M.; Wu, W.; Woo, E. P. *Science* **2000**, *290,* 2123. Huitema, H. E. A.; Gelinck, G. H.; van der Putten, J. B. P. H.; Kuijk, K. E.; Hart, C. M.; Cantatore, E.; Herwig, P. T.; van Breemen, A. J. M. M.; de Leeuw, D. M. *Nature* **2001**, *414*, 599. Babel, A.; Jenekhe, S. A. *J. Am. Chem. Soc.* **2003**, *125*, 13656.
(3) Bader, M. M.; Custelcean, R.; Ward, M. D. *Chem. Mater.* **2002**, *15*, 616. Facchetti, A.; Mushrush, M.; Katz, H. E.; Marks., T. J. *Adv. Mater.* **2003**, *15*, 33. Chesterfield, R. J.; Newman, C. R.; Pappenfus, T. M.; Ewbank, P. C.; Haukaas, M. H.; Mann, K. R.; Miller, L. L.; Frisbie, C. D. *Adv. Mater.* **2003**, *15*, 1279. Halik, M.; Klauk, H.; Zschieschang, U.; Schmid, G.; Ponomarenko, S.; Kirchmeyer, S.; Weber, W. *Adv. Mater.* **2003**, *15*, 91. Facchetti, A.; Yoon, M.-H.; Stern, C. L.; Katz, H. E.; Marks, T. J. *Angew. Chem.* **2003**, *115*, 4030. Horowitz, G.; Hajlaoui, M. E. *Adv. Mater.* **2002**, *12*, 1046. Hotta, S.; Goto, M. *Adv. Mater.* **2002**, *14*, 498. Videlot, C.; Ackermann, J.; Blanchard, P.; Raimundo, J.-M.; Frere, P.; Allain, M.; de Bettignies, R.; Levillain, E.; Roncali, J. *Adv. Mater.* **2003**, *15*, 306. Facchetti, A.; Deng, Y.; Wang, A.; Koide, Y.; Sirringhaus, H.; Marks, T. J.; Friend, R. H. *Angew. Chem.* **2000**, *112,* 4721.
(4) Horowitz, G.; Bachet, B.; Yassar, A.; Lang, P.; Demanze, F.; Fave, L.-L.; Garnier, F. *Chem. Mater.* **1995**, *7*, 1337.

10.1021/cm049686a CCC: $27.50
Published on Web 06/26/2004

in the β-position of the conjugated backbone leads to only a slight increase of solubility (less than 1 g/L).[6] On the other hand, introduction of larger hexyl groups in the β-position makes OTs extremely soluble but, simultaneously, suppresses the field-effect (FE) mobility, at least in some cases described in the literature.[5]

Garnier at al. have compared the FE mobility and solid-state organization of 6T, α,ω-hexyl-6T (α,ω-DH6T), and a mixture of regioisomers of β,β'-substituted 6T (*regioirregular* β,β'-DH6T).[5] It has been reported that α,ω-DH6T has a melting point of 290 °C, forms a nearly crystalline layered film, and possesses an excellent FE mobility. The melting point of 6T is 280 °C, it forms less ordered films, and it shows lower FE mobility compared with α,ω-DH6T by a factor of 25. It has also been demonstrated that OTs and polythiophenes[7] exhibit high mobility and conductivity if they adopt a fully planar molecular conformation, a dense and ordered molecular packing, and a preferred orientation of molecules essentially normal to the substrate to maximize the flow of charges from source to drain electrodes.[3−5,7] In sharp contrast to α,ω-DH6T, an extremely soluble and easily melted (80 °C) regioirregular β,β'-DH6T forms completely amorphous films and displays very low mobility below the detection limit.[5] Nevertheless, it remains unclear whether such a big difference in the properties of homologous systems originates from the *position of the alkyl groups* or from *irregularity* of the structure. The synthesis of the regiochemically pure β-substituted 6T has been described recently,[8,9] but to the best of our knowledge, the FE mobility has not been presented.

Here we report on the improved synthesis and charge carrier mobility of the 4′,3‴′-dihexyl-2,2′;5′,2″;5″,2‴;5‴,2⁗;5⁗,2⁗′-sexithiophene (β,β'-DH6T). The sum of charge carrier mobilities of β,β'-DH6T measured by the pulse-radiolysis time-resolved microwave conductivity (PR-TRMC)[10]technique was found to be $\sum\mu_{min} = 3.9 \times 10^{-3}$ cm^2 V^{-1} s^{-1}, which is 1 order of magnitude less than the PR-TRMC mobility found for α,ω-DH6T.[11] The charge carrier mobilities obtained by PR-TRMC measurements should be considered as a measure of the trap-free mobility. The FE mobility of β,β'-DH6T was found to be on the order of 10^{-5} cm^2 V^{-1} s^{-1}. To understand the reason for such poor macroscopic electrical properties, we systematically studied the conformation and the molecular packing of β,β'-DH6T by means of UV−vis spectroscopy, scanning electron microscopy (SEM), atomic force microscopy (AFM), and X-ray techniques. We found that β,β'-DH6T is readily soluble in common organic solvents and forms smooth and uniform films by spin-coating. Absorption spectra of the β,β'-DH6T spin-cast film indicate the planar conformation of the aromatic backbone. SEM and AFM reveal the formation of an ordered lamellar phase. A single-crystal X-ray study supports the planar conformation of the β,β'-DH6T backbone in the solid state and reveals a herringbone molecular packing typical for unsubstituted and α,ω-substituted oligothiophenes. Nevertheless, there are several important differences in the molecular packing of β,β'-DH6T, 6T, and α,ω-DH6T. β,β'-DH6T exhibits less dense crystalline packing than 6T and α,ω-DH6T, as seen by larger distances between the centers of neighbor OT molecules.[4,5] In contrast to the almost upright orientation of α,ω-DH6T and 6T molecules against the substrate (tilt angle about 68°), the long axis of β,β'-DH6T molecules and the surface plane form an angle of ~20° as revealed by X-ray diffraction studies of β,β'-DH6T films. While the crystalline structure of 6T and α,ω-DH6T "allows" the current to flow through molecular stacks along two self-perpendicular directions, the crystalline structure of β,β'-DH6T suppresses the charge transport in all directions.

Results

Synthesis. β,β'-DH6T was synthesized by a modified method derived from previously reported procedures by Hadziioannou at al.[9] and Zimmer at al.[12] Dihexylquaterthiophene **2** was synthesized by the Kumada coupling[13] of 2 equiv of the Grignard reagent **1** with 5,5-dibromothiophene (Scheme 1). The isomerically pure β,β'-DH6T was synthesized by the cross-coupling of the Grignard reagents of 2-bromothiophene with dibromide **3** in 42% overall yield starting from commercially available 3-hexylthiophene.

β,β'-DH6T shows good solubility in common organic solvents. For example, the solubility in $CHCl_3$ at 20 °C is 10 g/L and near 50 g/L at 35 °C. Taking into account a close relationship between the purity of semiconductive materials and their charge transport properties, the desired product was purified carefully. The crude β,β'-DH6T was purified twice by column chromatography on silica gel and subsequently crystallized 3−5 times from chloroform. Importantly, we did not find any detectable impurities after the first crystallization, as indicated by NMR spectroscopy and MALDI-TOF.

Electrical Characterization. To investigate the electronic conduction behavior of the organic semiconductors, thin films of the materials were deposited onto test vehicles based on a bottom gate FET design. These test vehicles employed the commonly known Si/SiO_2 approach for the gate electrode and the gate dielectrics with a gate oxide thickness of 90 and 185 nm, yielding a gate capacitance of 380 and 190 pF/mm^2, respectively. Gold source/drain contacts of 150 nm gold were deposited onto the SiO_2 using lift-off-patterning. Out of a

(5) Garnier, F.; Yassar, A.; Hajlaoui, R.; Horowitz, G.; Deloffre, F.; Servet, B.; Ries, S.; Alnot, P. *J. Am. Chem. Soc.* **1993**, *115*, 8716.
(6) Barbarella, G.; Zambianchi, M.; Antolini, L.; Ostoja, P.; Maccagnani, P.; Bongini, A.; Marsegilia, E. A.; Tedesco, E.; Gigli,G.; Cingolani, R. *J. Am. Chem. Soc.* **1999**, *121*, 8920.
(7) Sirringhaus, H.; Brown, P. J.; Friend, R. H.; Nielsen, M. M.; Bechgaard, K.; Langeveld-Voss, B. M. W.; Spiering, A. J. H.; Janssen, R. A. J.; Meijer, E. W.; Herwig, P.; de Leeuw, D. M. *Nature* **1999**, *401,* 685.
(8) Bäuerle, P.; Pfau, F.; Schlupp, H.; Würthner, F.; Gaudl, K.-U.; Caro, M. B.; Fischer, P. *J. Chem. Soc., Perkin Trans.* **1993**, *2*, 489. Bäuerle, P.; Segelbacher, U.; Gaudl, K.-U.; Huttenlocher, D.; Mehring, M. *Angew. Chem.* **1993**, *32*, 76.
(9) Herrema, J. K.; Wildeman, J.; van Bolhius, F.; Hadziioannou, G. *Synth. Met*. **1993**, *60*, 239.
(10) (a) Warman, J. M.; Gelinck, G. H.; de Haas, M. P. *J. Phys.: Condens. Matter* **2002**, *14*, 9935. (b) Krebs, F. C.; Jorgensen, M. *Macromolecules* **2003**, *36*, 4374.
(11) Wegewijs, B.; Haas, M. P.; de Leeuw, D. M.; Wilson, R.; Sirringhaus,H. *Synth. Met*. **1999**, *101*, 534. Haas, M. P.; van der Laan, G. P.; Wegewijs, B.; de Leeuw, D. M.; Bäuerle, P.; Rep, D. B. A.; Fichou, D. *Synth. Met*. **1999**, *101*, 524.
(12) Burkhardt, C. V. P.; Shabana, R.; Cunningham, D. D.; Mark, H. B.; Zimmer, H. *Phosporus, Sulfur, Silicon* **1989**, *46*, 153.
(13) Tamao, K.; Komada, S.; Nakajima, I.; Kumada, M.; Minato, A.; Suzuki, K. *Tetrahedron* **1982**, *38*, 3347.

Scheme 1. Synthesis of β,β′-DH6T

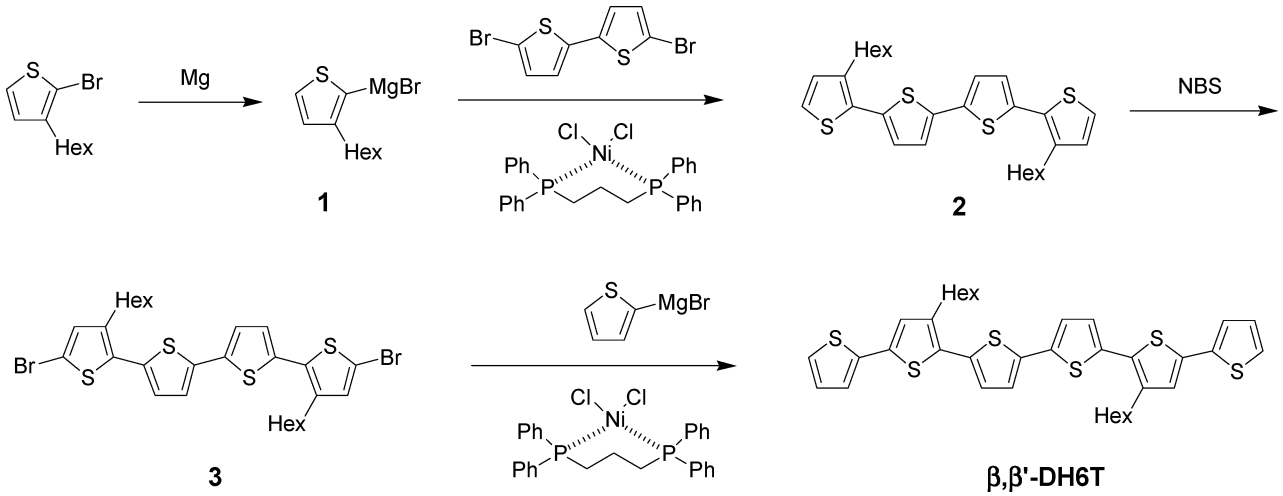

variety of transistor test patterns, single linear and octagonal wide channel transistors with channel lengths of 15−50 μm and channel widths of 1000−3000 μm were chosen for material evaluation. Films (30−80 nm thick) of β,β′-DH6T were deposited by spin-coating from chloroform solution. Output and transfer characteristics of the transistors were measured using a prober with W-tips (PM5, Suess) in a dark box and a two-SMU measuring setup (K2400/K6430, Keithley) controlled by PC software. This allows the gate leakage to be checked and taken into account with the measured drain currents. From the transfer characteristics the FET mobilites were calculated in both the linear and the saturation regions. For this overall estimation of the semiconductor material properties the two values have been averaged with a single mean. The completed transistor chips after semiconductor deposition were stored under argon until electric measurements; the transistor behavior itself was measured under a nitrogen flow to prevent interaction of the uncovered organic semiconductor with the humid atmosphere. The measured drain currents were corrected using a simple two-path-distribution model for the gate currents. In the best case we obtained p-channel MOS−FET behavior with an FET mobility up to 2×10^{-5} cm^2 V^{-1} s^{-1} and threshold voltages between +10 and −5 V. Figure 1 gives output characteristics of a transistor with an octagonal channel of 15 μm × 3000 μm on a 185 nm SiO_2 gate dielectric.

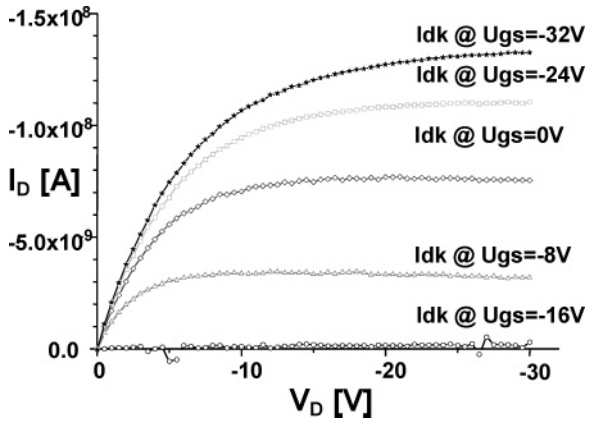

Figure 1. Drain current I_D versus drain voltage V_D at different gate voltages (V_G).

The intrinsic charge transport properties of β,β′-DH6T were measured by the PR-TRMC technique. Charge carriers are produced in a powder sample by irradiation with high-energy (10 MeV) electrons, and the resulting change in conductivity is monitored with R-band microwaves (26−40 GHz). The technique has been described in detail in the literature by Warman et al.[10a] The setup used for the experiments reported here has been described in ref 10b. The PR-TRMC method does not rely on electrical contacts being made and thus avoids barrier problems between the electrodes and the sample, at domain boundaries and between crystallites. The sum of charge carrier mobilities was determined to be $\sum\mu_{min} = 3.9 \times 10^{-3}$ cm^2 V^{-1} s^{-1} (on the basis of a pair formation energy of 25 eV) (Figure 2), which is slightly less than the mobility of regioirregular β,β′-DH6T and 10 times less than the mobility of α,ω-DH6T.[11] To find the reason for the poor electrical properties, we performed an extensive study of β,β′-DH6T by means of UV−vis spectroscopy, SEM, AFM, and X-ray techniques.

UV−Vis Spectroscopy. UV−vis spectroscopy has been proven as a sensitive tool for the investigation of conformational changes and intermolecular interactions of conjugated systems in both solution and the solid state.[14] In chloroform solution β,β′-DH6T exhibits a broadened absorption band with $\lambda_{max} = 418$ nm (Figure 3). The absorption shows no fine structure and is attributed to the $\pi-\pi^*$ transition of isolated conforma-

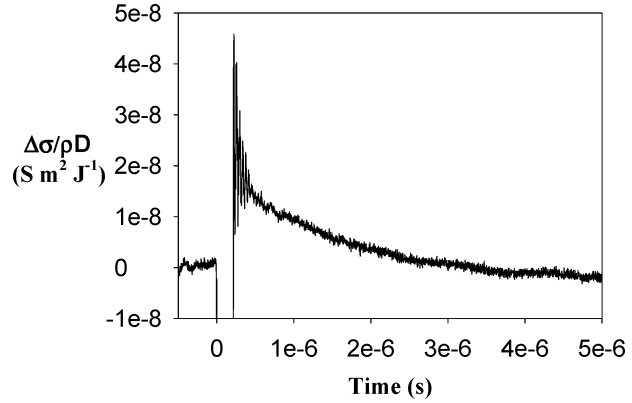

Figure 2. A dose-normalized conductivity transient for β,β′-DH6T as obtained from PR-TRMC measurements using a 200 ns pulse of 10 MeV electrons.

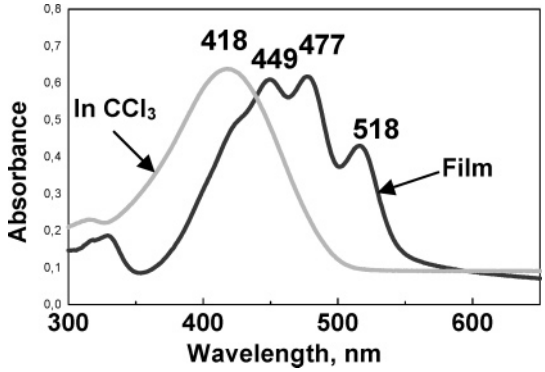

Figure 3. UV−vis spectra of the β,β'-DH6T film and the β,β'-DH6T solution in chloroform.

tionally disordered molecules. In solid films of β,β'-DH6T obtained by spin-coating we observed a red shift of 49 nm ($\lambda_{max} = 477$ nm) and the appearance of fine structure (signals at 449 and 518 nm). We ascribe this to the planarization of the conjugated system and a formation of ordered structures. The fine structure is ascribed to a progression of the $\pi-\pi^*$ transition related to the C=C vibronic transition.[14]

Morphology of β,β'-DH6T. It was previously demonstrated that the efficiency of charge transport is directly related to the long-range packing of molecules in the semiconducting film.[15] Therefore, we investigated the morphology of the β,β'-DH6T films by optical microscopy, SEM, and AFM.[16] Thin films were prepared by spin-coating from β,β'-DH6T solution in chloroform onto the device as described in the Experimental Section. We found that β,β'-DH6T forms smooth and homogeneous films on scales from several hundreds of micrometers to several hundreds of nanometers. Figure 4a shows the optical micrograph of the device, which reveals a polycrystalline nature of the film.

As shown by SEM investigations the morphology of β,β'-DH6T films strongly depends on the temperature at which samples are prepared. We found that spin-coating from β,β'-DH6T solution in chloroform *at room temperature* results in films consisting of random oriented needle crystals with a grain size of about 1 μm. In contrast, lamellar structures were formed when β,β'-DH6T was deposited at 40 °C. Figure 4 illustrates an intermediate case, the coexistence of both phases formed upon the deposition from the solution at 30 °C. Similar "switching" of the film morphology between a "single-crystal phase" and a "thin-film phase" by deposition conditions and strong preference of the "thin-film phase"

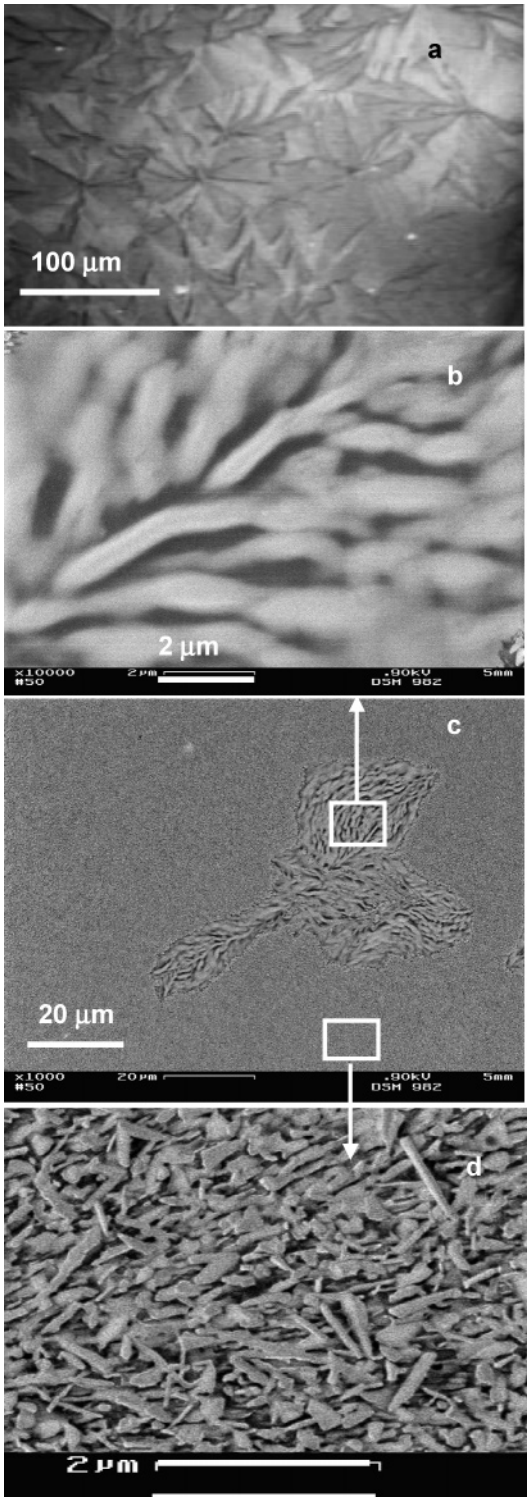

Figure 4. Optical (a) and SEM (b−d) micrographs of a β,β'-DH6T film deposited onto the device.

for good charge mobility have been previously demonstrated for pentacene.[17]

AFM studies allowed us to gain deeper insight into the fine structure of β,β'-DH6T films. Figure 5 shows AFM images of different parts of the device with β-DH6T deposited at 40 °C. They reveal the formation of the uniform lamellar networks of β,β'-DH6T on the gold electrodes as well as on the SiO_2 surfaces between

(14) Sundberg, M.; Inganäs, O.; Stafström, S.; Gustafsson, G.; Sjögren, B. *Solid State Commun.* **1989**, *71*, 435. Brustolin, F.; Goldoni, F.; Meijer, E. W.; Sommerdijk, N. A. J. M. *Macromolecules* **2002**, *35*, 1054. Kiriy, N.; Jähne, E.; Adler, H.-J.; Schneider, M.; Kiriy, A.; Gorodyska, G.; Minko, S.; Jehnichen, D.; Simon, P.; Fokin, A. A.; Stamm, M. *Nano Lett.* **2003**, *3*, 707. Apperloo, J. J.; Janssen, R. A. J.; Malenfant, P. R. L.; Frechet, J. M. J. *Macromolecules* **2000**, *33*, 7038. Levesque, I.; Bazinet, P.; Roovers, J. *Macromolecules* **2000**, *33*, 2952.

(15) Katz, H.; Lovinger, A. J.; Laquindanum, J. G. *Chem. Mater.* **1998**, *10*, 457.

(16) Magonov, S. N.; Reneker, D. H. *Annu. Rev. Mater. Sci.* **1997**, *27*, 175. Tsukruk, V. V.; Reneker, D. H. *Polymer* **1995**, *36*, 1791−1808. Minko, S.; Kiriy, A.; Gorodyska, G.; Stamm, M. *J. Am. Chem. Soc.* **2002**, *124*, 3218. Minko, S.; Kiriy, A.; Gorodyska, A.; Stamm, M. *J. Am. Chem. Soc.* **2002**, *124*, 10192. Kiriy, A.; Gorodyska, G.; Minko, S.; Jaeger, W.; Stepanek, P., Stamm, M. *J. Am. Chem. Soc.* **2002**, *124*, 13454. Kiriy, A.; Gorodyska, G.; Minko, S.; Jaeger, W.; Stepanek, P., Stamm, M. *J. Am. Chem. Soc.* **2003**, *124*, 13454.

(17) Dimitrakopoulos, C. D.; Brown, A. R.; Pomp, A. *J. Appl. Phys.* **1996**, *80*, 2501.

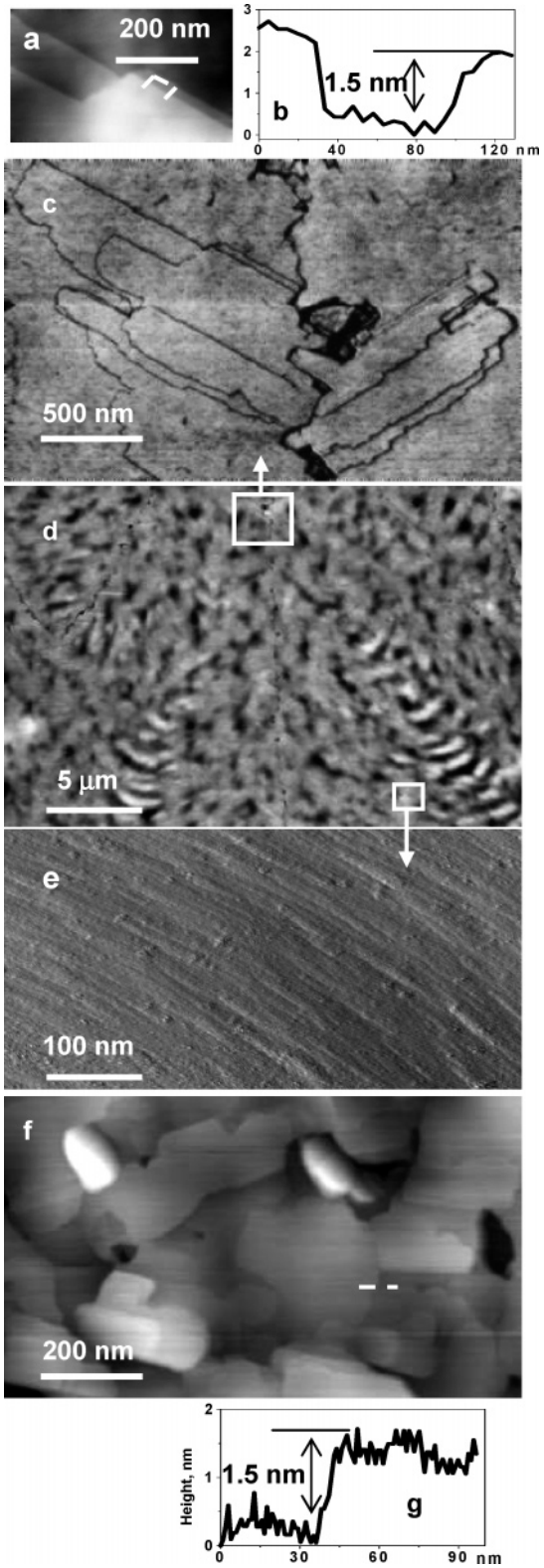

Figure 5. Representative AFM images and cross-sections of a β,β′-DH6T film deposited onto the device by spin-coating at 40 °C: topography (a), phase images (c), and cross-section (b) of terrace structures formed on defects; large-scale (d) and small-scale (e) topography images of lamellar structures; topography image (f) and cross-section (g) of terraces of a β,β′-DH6T film formed on the hydrophobic surface (BCB).

them (Figure 5d). A similar lamellar morphology is also observed in the high-resolution AFM image (Figure 5e). This type of scaling behavior of the thin-film morphology

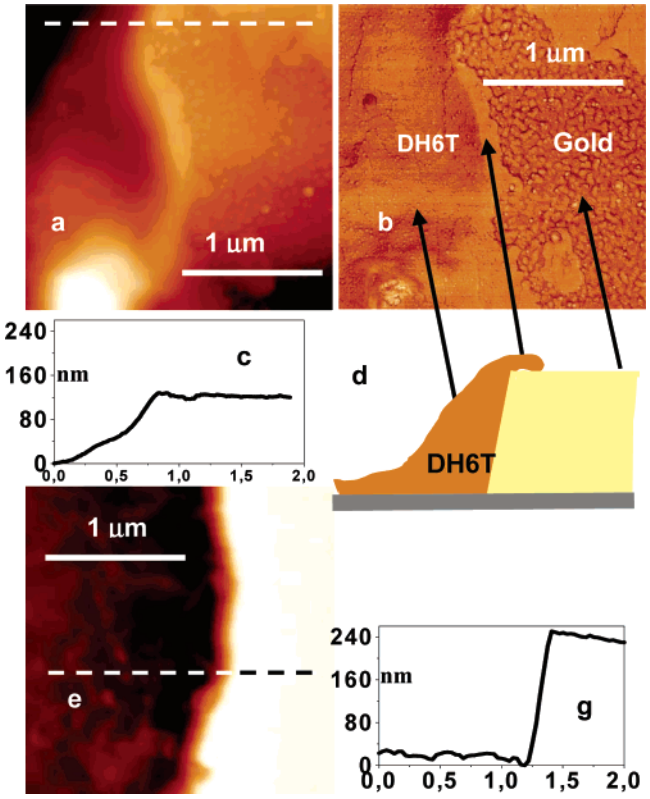

Figure 6. Representative AFM images and cross-sections of the device coated by β,β′-DH6T in the area of the contact—topography image (a), phase image (b), and cross-section (c)—and of the uncoated device—topography image (e) and cross-section (g). The schematic profile of the coated device corresponded to the image (b) and reflected a good contact between the gold electrode and the β,β′-DH6T film (d).

termed self-affinity is general for OTs, and has been previously found in unsubstituted 6T and 5T films.[18]

AFM revealed the formation of small flat terrace crystallites grown on boundaries between large lamella domains (Figure 5a−c). As shown in Figure 5a, the smallest step observed between adjacent terraces is about 1.5 nm, which is less than the longest axis of the β,β′-DH6T molecule (molecular length ~2.6 nm). Only flat terrace structures was found when β,β′-DH6T was deposited onto the hydrophobic polymer film (benzocyclobutene, BCB). As in the previous case, the smallest step between adjacent terraces is about 1.5 nm (Figure 5f,g).

Taking into account the great influence of the contact quality on the electrical characteristics of the device, the areas around gold electrodes were investigated more carefully. Figure 6e shows an AFM image of the edge of the uncoated device with the step height about 240 nm. The deposition of β,β′-DH6T results in the decrease of the height of the step up to 100 nm. The areas corresponding to β,β′-DH6T and gold electrode are clearly distinguishable from the phase image (Figure 6b). Although, the electrode surface is not completely covered, β,β′-DH6T homogeneously covers *the edge of the electrode* from the foot to the top, as schematically shown in Figure 6d. It should be noted that an indica-

(18) Melucci, M.; Gazzano, M.; Barbarella, G.; Cavallini, M.; Biscarini, F.; Maccagnani, P.; Ostoja, P. *J. Am. Chem. Soc.* **2003**, *125*, 10266.

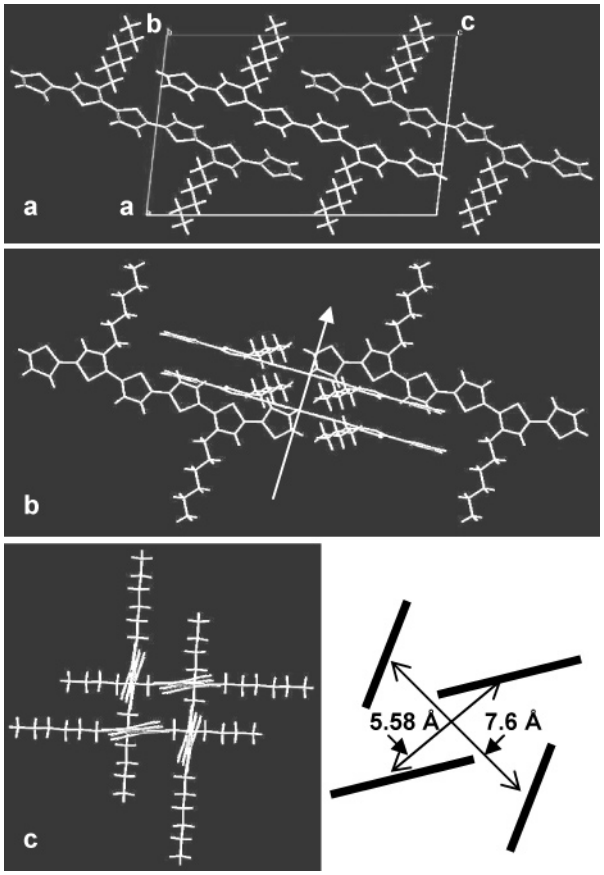

Figure 7. Representation of the crystal packing of β,β'-DH6T: the view along the *b* axis (a); the view in the plane of two stacked β,β'-DH6T molecules as shown by the white arrow (b); the view in the plane of the aromatic backbone along the molecular long axis (c).

tion of contacts based on visual inspection, in general, does not ensure that the film and electrodes form ohmic contacts.

X-ray Techniques. Although structures of several β,β'-substituted 6T single crystals have been reported, there are no structural data for films of β,β'-DH6T. Exact knowledge of the crystalline structure and the molecular orientation in OT films is important for better understanding and tuning of their charge transport properties. Figure 7 shows the crystal structure of β,β'-DH6T with a monoclinic arrangement and the space group $P2_1/c$. The thiophene rings are nearly planar. The dihedral angles between the thiophene rings are 3−4°, which is very close to the values for unsubstituted 6T. Hexyl chains adopt a planar zigzag conformation.[19]

β,β'-DH6T molecules display a herringbone arrangement as seen from Figure 7c, which presents a view of the unit cell in the plane of the thiophene backbone along the molecular long axis. Such a motif is typical for the packing for planar conjugated aromatics such as acenes and OTs.[20] Two β,β'-DH6T molecules of the unit cell are stacked as in the 6T crystal, and the distance between the centers of neighboring molecules is 5.58 Å. Two other molecules of the unit cell are considerably shifted with respect to each other, so that only the last aromatic ring of one molecule is projected onto the first ring of the other one and the distance between the centers of this rings is equal to 7.6 Å (Figure 7b,c).

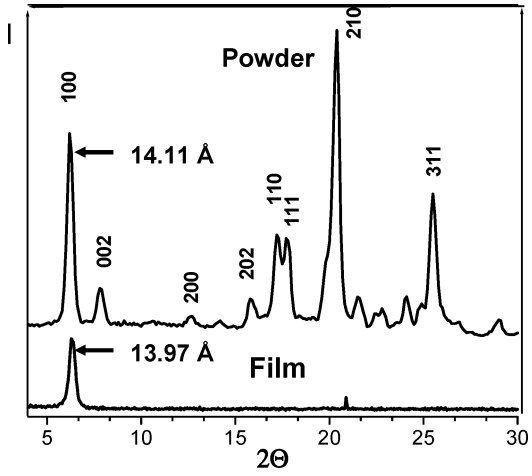

Figure 8. X-ray diffractograms of a powder (top line) and a 110 nm thick film (bottom line) of β,β'-DH6T.

To investigate the orientation of β,β'-DH6T molecules in a thin film, we performed X-ray investigation of the film. Figure 8 (bottom line) shows the X-ray pattern of a 110 nm β,β'-DH6T film deposited by spin-coating from chloroform solution at 40 °C. The diffractogram contains only the strong reflection at $2\theta = 6.32°$ (13.97 Å), which is close to the *a*-axis of the unit cell (a = 13.88 Å). Similar angular positions of the low-angle reflection might indicate that the film, powder, and single crystal exhibit the same crystalline structure. The absence of all other reflections in the film indicates the strong orientation of β,β'-DH6T molecules as shown in Figure 8. Thus, in contrast to the almost upright orientation of α,ω-DH6T and 6T molecules against the substrate (tilt angle 67−68°), the long axis of β,β'-DH6T molecules and its projection onto the surface plane form an angle of about 20°. Such a result is in agreement with AFM data: the reflection at 6.32° corresponding to the interlayer *d* spacing of 13.97 Å is close to the smallest thickness of terraces observed by AFM (about 1.5 nm, Figure 5). It was previously shown that the molecular orientation and electric transport properties in some cases are dependent on the underlying surface. We investigated β,β'-DH6T films deposited onto a polystyrene film, and onto the substrate hydrophobized by octadecyldimethylchlorosilane. We found no difference in the film morphology, crystalline structure, and molecular orientation, as revealed by AFM and X-ray studies.

Discussion and Conclusions

β,β'-DH6T forms smooth and well-ordered films of planar molecules packed in a herringbone fashion. From this point of view, such an organization of β,β'-DH6T is similar to the organization observed for other OTs displaying excellent charge mobilities. Despite the structural similarity, β,β'-DH6T exhibits poor electrical

(19) Crystal data for the β,β'-DH6T single crystal grown upon slow evaporation from the chloroform solution are given in Table S1 (see the Supporting Information). The atomic numbering scheme, the positional parameters, and the bond distances and angles are given in Tables S2−4. The structural data are consistent with previously reported data: Sato, T.; Fujitsuka, M.; Shiro, M.; Tanaka, K. *Synth. Met.* **1998**, *95*, 143.

(20) Cornil, J.; Calbert, J. P.; Bredas, J. L. *J. Am. Chem. Soc.* **2001**, *123*, 1250.

properties. To understand the reason for such a striking difference in the properties of homologous compounds, we analyzed and compared their crystalline structures. There are several important differences in the molecular packing of β,β′-DH6T, α,ω-DH6T, and 6T. The unit cells of α,ω-DH6T and 6T consist of two pairs of molecules stacked along the long axis in two self-perpendicular planes. The distances between the centers of neighboring 6T molecules are 4.95 Å for one pair and 5.5 Å for the second pair.[5] In contrast, only one of the pairs of β,β′-DH6T molecules is stacked (the distance between the centers of neighboring β,β′-DH6T molecules is 5.58 Å), whereas the other two molecules are largely shifted with respect to each other and the distance between the centers of overlapped rings is 7.6 Å. On the other hand, the X-ray study of the β,β′-DH6T, α,ω-DH6T, and 6T films reveals their different molecular orientations. In contrast to the almost upright orientation of α,ω-DH6T and 6T molecules against the substrate (tilt angle 67−68°), which is favored for charge transport, β,β′-DH6T molecules are oriented almost parallel to the surface (the β,β′-DH6T long axis and the surface plane form an angle of about 20°). Thus, assuming that the maximal charge transport is realized in the direction perpendicular to the plane of the thiophene rings,[3−5] the crystalline structures of 6T and α,ω-DH6T favor the current flow in two almost self-perpendicular directions.[5] In contrast, the unit cell of β,β′-DH6T is strongly anisotropic, and only one possibility is "allowed" for current to pass through the β,β′-DH6T crystal as shown by the arrow in Figure 7b. This direction is virtually perpendicular to the direction of the applied potential. In contrast to that of the 6T crystal, the molecular packing of β,β′-DH6T also impedes the charge transport in the direction parallel to the molecular long axis. As seen from Figure 7a, although all β,β′-DH6T molecules are aligned along the molecular long axis, they are isolated from each other by nonconductive alkyl chains. Such a strong dependence of charge transport properties on the orientation of β,β′-DH6T crystalline domains is not so important for PR-TRMC measurements, which provide information on the charge carrier mobility over small distances (over a few nanometers). The PR-TRMC method allows for the estimation of the average carrier mobility assuming that the crystallites in the powdered sample are randomly oriented. We propose following a similar explanation for the observed discrepancy between the FEM mobility and the PR-TRMC mobility. The carrier transport properties as measured by PR-TRMC are over distances much smaller than those of the ordered domains in the crystals and can thus be considered as the maximum trap-free in-domain mobility values. This can easily account for the much lower carrier mobility values observed for the FEM measurements, which rely on carrier transport over macroscopic distances through many domains that may not be oriented for optimal carrier transport.

Experimental Section

General Procedures. All chemicals were purchased from Aldrich and used as received. ^{1}H and ^{13}C NMR spectra were recorded on a Bruker DRX-500 spectrometer at frequencies of 500.13 MHz (^{1}H) and 125.76 MHz (^{13}C) with tetramethylsilane as an internal standard. UV−vis measurements were carried out using a Perkin-Elmer Lambda 19 UV−vis spectrometer. MALDI-TOF MS was performed on a Bruker Biflex IV mass spectrometer. For AFM measurements we used a multimode AFM instrument (Digital Instruments, Santa Barbara) operating in the tapping mode. Silicon tips with a radius of 10−20 nm, a spring constant of 0.3 N/m, and a resonance frequency of 250−300 kHz were used. SEM images were taken with a Gemini microscope (Zeiss, Germany). Crystallographic data of the single crystal were collected at 293 K on a STOE IPDS with Mo Kα radiation (λ = 0.71073 Å). The structure was solved by direct methods using SHELXS-97[21] and was refined by the full-matrix least-squares method with SHELXS-93.[22] XRD diagrams of powders were recorded in the transmission mode using X-ray diffractometer P4 (Siemens AG Karlsruhe) with Cu Kα radiation (monochromatization by the primary graphite crystal; primary pinhole ∅ = 0.5 mm; detector distance 12 cm). XRD diagrams of the films were recorded in the reflection mode using XRD 3003 (Seifert-FPM Freiberg/Sa.) (monochromatization by the primary multilayer system).

3,3‴-Dihexyl-2,2′;5′,2″;5″,2‴-tetrathienyl (2). To a solution of 3.24 g (0.01 mol) of 5,5-dibromothiophene and 60 mg of $NiCl_2$(dppp) in 100 mL of ether was added dropwise a 2-thienylmagnesium bromide/ether solution (0.022 mol). The resulting solution was stirred at room temperature overnight, hydrolyzed with ice cold 1 N HCl, and then extracted with ether. The organic layer was dried over $MgSO_4$ and evaporated. The residue was purified by flash chromatography, and 3.68 g (74%) of **2** was obtained. ^{1}H NMR: δ 7.171 (d, J = 5.2 Hz, 1H), 7.12 (d, J = 3.7 Hz, 1H), 7.015 (d, J = 3.7 Hz, 1H), 6.93 (d, J = 5.2 Hz, 1H), 2.776, (t, J = 7.8 Hz, 2H), 1.64 (m, 2H), 1.35 (m, 6H), 0.88 (m., 3H). UV−vis ($CHCl_3$): λ_{max} = 382.4 nm.

5,5‴-Dibromo-3,3‴-dihexyl-2,2′;5′,2″;5″,2‴-tetrathienyl (3). A 2.63 g (0.015 mol) sample of bromosuccinimide (NBS) was added to the solution of **2** (3.68 g, 0.0074 mol) in 30 mL of a chloroform−acetic acid mixture (50/50 v/v) in the absence of light, under an argon atmosphere, at temperature 0 °C. The mixture was allowed to reach room temperature, stirred overnight, and hydrolyzed with 50 mL of ice−water and the aqueous phase extracted with chloroform. The combined extracts were washed with water, dried ($MgSO_4$), and concentrated. The residue was purified by flash chromatography to give 4.48 g (0.0068 mol) of dibromide **3** (92% yield). ^{1}H NMR (400 MHz, $CDCl_3$): δ 7.08 (d, J = 3.8 Hz, 1H), 6.94 (d, J = 3.8 Hz, 1H), 6.88 (s, 1H), 2.70 (t, J = 7.7 Hz, 2H), 1.604 (m, 2H), 1.298 (m, 6H), 0.864 (m, 3H).

2,2′;5′,2″;5″,2‴;5‴,2⁗;5⁗,2⁗′-Sexithiophene (β,β′-DH6T). This compound was prepared in a manner similar to that of **2** from 3.28 g (0.005 mol) of **3**, 30 mg of $NiCl_2$(dppp), and 0.001 mol of 2-thienylmagnesium bromide. After 20 h of reaction time, a deep orange precipitate was filtered off and dried under reduced pressure (yield 2.7 g, 82%). The crude product was twice purified by column chromatography (silica gel, hexane) and then 3−5 times crystallized from chloroform. ^{1}H NMR (400 MHz, $CDCl_3$): δ 7.209 (dd J_1 = 5 Hz, J_2 = 0.8 Hz, 1H), 7.163 (dd, J_1 = 3.5 Hz, J_2 = 0.8 Hz, 1H), 7.127 (d, J = 3.8 Hz, 1H), 7.035 (d, J = 3.8 Hz, 1H), 7.014 (t, J_1 = 5 Hz, J_2 = 3.5 Hz, 1H), 7.011 (s, 1H), 2.76 (t, 2H), 1.6−1.3 (m, 8H), 0.86 (m, 3H). ^{13}C NMR ($CDCl_3$, ppm, TMS): δ 140.48, 137.12, 136.68, 135.22, 135.01, 129.30, 127.86, 126.66, 126.35, 124.42, 123.91, 123.64, 31.65, 30.45, 29.50, 29.23, 22.61, 14.10. MS: *m/e* 662 ($M^{\bullet+}$). UV−vis ($CHCl_3$): λ_{max} = 418 nm. Mp: 128.78 °C.

Sample Preparation. Highly polished Si wafers (obtained from Wacker-Chemitronics) were first cleaned in an ultrasonic bath three times for 5 min with dichloromethane, placed in a cleaning solution (prepared from NH_4OH and H_2O_2) for 1 h, and finally rinsed several times with Millipore water (18 MΩ cm). β,β′-DH6T was deposited onto a Si wafer by spin-coating (2000 rotations/min) from a 2−5% solution in $CHCl_3$. The

(21) Sheldrick, G. M. *SHELXS-97, program for X-ray crystal structure solution*; University of Göttingen: Göttingen, Germany 1997.
(22) Sheldrick, G. M. *SHELXS-93, program for X-ray crystal structure refinement*; University of Göttingen: Göttingen, Germany 1993.

thickness of the resulting film was evaluated by ellipsometry (30−130 nm dependent on concentration). For hydrophobization freshly cleaned Si wafers were placed in a 2% solution of octadecyldimethylchlorosilane in $CHCl_3$ for a respective time (from 10 min to overnight), then rinsed with pure $CHCl_3$, and finally dried with an argon flux.

Acknowledgment. We thank Mrs. E. Kern for the SEM study, Dr. D. Kukling for MALDI-TOF MS measurements, and Dr. E. Jähne and Dr. K. Potje-Kamloth for helpful discussions. We are grateful for the financial support provided by the Deutsche Forschungsgemeinschaft (Project DFG-Sachb. AD 119/6-1, and DFG/CNRS German-French bilateral program, STA 324/13).

Supporting Information Available: Crystal data and structural results, atomic numbering scheme, atomic coordinates, equivalent isotropic displacement parameters for nonhydrogen atoms, and bond lengths and angles for β,β'-DH6T (CIF, PDF). This material is available free of charge via the Internet at http://pubs.acs.org. The crystal structure has also been deposited at the Cambridge Crystallographic Data Center and allocated the deposition number CCDC 232590.

CM049686A